Handbook of Clinical Neurology, Vol. 102 (3rd series)
Neuro-ophthalmology
C. Kennard and R.J. Leigh, Editors

Chapter 1

Anatomy and physiology of the afferent visual system

SASHANK PRASAD [1*] AND STEVEN L. GALETTA [2]

[1] *Division of Neuro-ophthalmology, Department of Neurology, Brigham and Women's Hospital, Harvard Medical School, Boston, MA, USA*

[2] *Neuro-ophthalmology Division, Department of Neurology, Hospital of the University of Pennsylvania, Philadelphia, PA, USA*

INTRODUCTION

Visual processing poses an enormous computational challenge for the brain, which has evolved highly organized and efficient neural systems to meet these demands. In primates, approximately 55% of the cortex is specialized for visual processing (compared to 3% for auditory processing and 11% for somatosensory processing) (Felleman and Van Essen, 1991). Over the past several decades there has been an explosion in scientific understanding of these complex pathways and networks. Detailed knowledge of the anatomy of the visual system, in combination with skilled examination, allows precise localization of neuropathological processes. Moreover, these principles guide effective diagnosis and management of neuro-ophthalmic disorders.

The visual pathways perform the function of receiving, relaying, and ultimately processing visual information. These structures include the eye, optic nerves, chiasm, tracts, lateral geniculate nucleus (LGN) of the thalamus, radiations, striate cortex, and extrastriate association cortices. Form follows function, and structural relationships often directly determine the underlying mechanisms of visual processing. The goal of this chapter is to describe in detail the anatomy and physiology of vision.

EYE

The eye is the primary sensory organ for vision, responsible for collecting light, focusing it, and encoding the first neural signals of the visual pathway. To reach the retina, light must pass through the ocular media, consisting of the tear film, cornea, anterior chamber, lens, and the posterior-chamber vitreous (Fig. 1.1). The corneal epithelium and stroma are transparent to permit passage of light without distortion (Maurice, 1970). The tear–air interface and cornea contribute more to the focusing of light than the lens does; unlike the lens, however, the focusing power of the cornea is fixed. The ciliary muscles dynamically adjust the shape of the lens in order to focus light optimally from varying distances upon the retina (accommodation). The total amount of light reaching the retina is controlled by regulation of the pupil aperture. Ultimately, the visual image becomes projected upside-down and backwards on to the retina (Fishman, 1973).

The majority of the blood supply to structures of the eye arrives via the ophthalmic artery, which is the first branch of the internal carotid artery (Hayreh, 2006). The ophthalmic artery enters the orbit via the optic canal, traveling beside the optic nerve. It then gives rise to two groups of vessels: those supplying the globe (including the central retinal artery, the muscular artery, the anterior ciliary arteries, and the long and short posterior ciliary arteries) and those supplying other orbital structures (including the lacrimal artery, supraorbital artery, ethmoidal arteries, frontal artery, and nasal artery). There are minor contributions from collateral vessels that originate in the external carotid arteries (via the infraorbital artery and the orbital branch of the middle meningeal artery). The patterns of blood supply to the eye and orbit can be quite complex, with tremendous variation between individuals (Meyer, 1887; Hayreh, 2006).

RETINA

When light reaches the retina, its energy is converted by retinal photoreceptors into an electrochemical signal that is then relayed by neurons. To arrive at the

*Correspondence to: Sashank Prasad, MD, Department of Neurology, Division of Neuro-Ophthalmology, Brigham and Women's Hospital, Harvard Medical School, Boston, MA, USA. Tel: (617) 732-7432, Fax: (617) 732-6083, E-mail: SPrasad2@partners.org

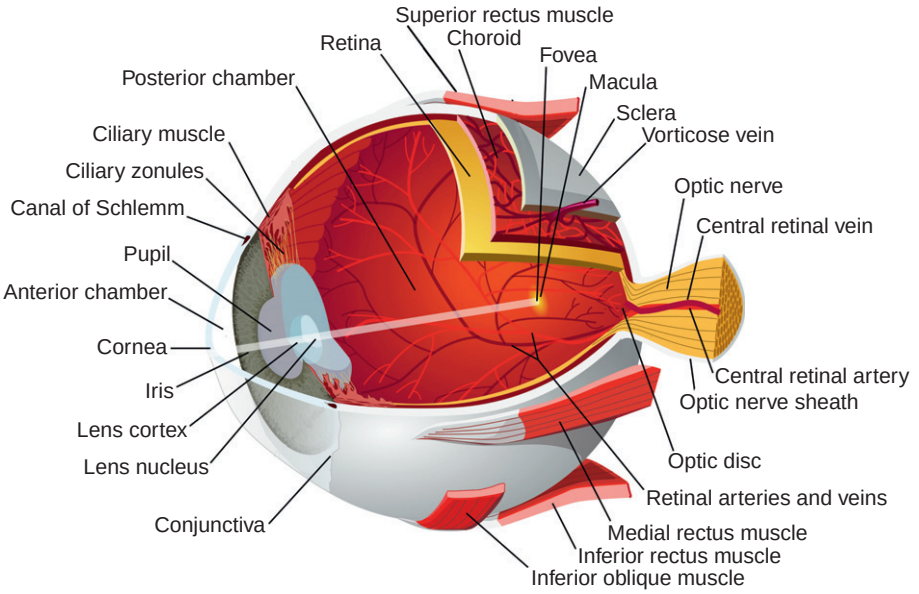

Fig. 1.1. The eye. Light passes through the anterior chamber, the lens, and the posterior chamber, and is then focused upside-down and backwards upon the retina.

photoreceptors, light must first pass through transparent inner layers of the neurosensory retina, comprised of the nerve fiber layer, ganglion cells, amacrine cells, and bipolar cells (Fig. 1.2). Immediately outside the photoreceptor layer is the retinal pigment epithelium (RPE). The RPE provides structural and metabolic support for the photoreceptors, primarily through the vital function of vitamin A metabolism (Wald, 1933). In addition, the RPE absorbs any intraocular light that has passed through the photoreceptor layer; this reduces

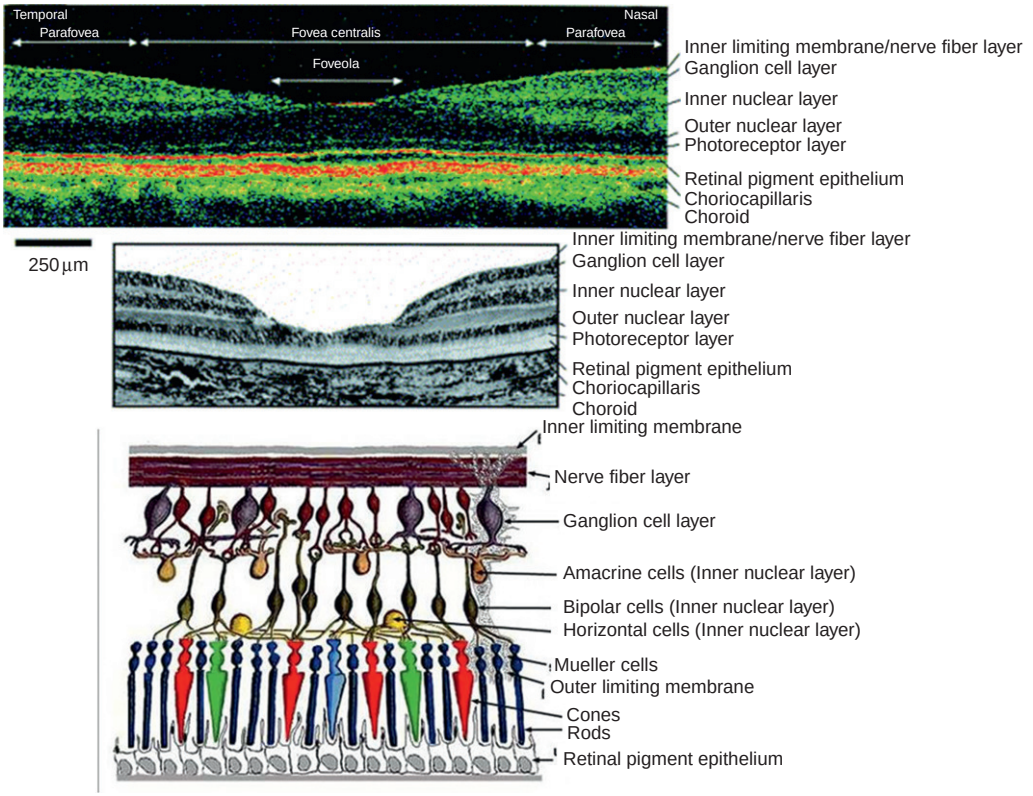

Fig. 1.2. Structures of the neurosensory retina. Top, high-resolution optical coherence tomography. Middle, histological section. Bottom, schematic depiction of retinal layers. (Adapted and reprinted with permission from Jaffe and Caprioli (2004), and www.webvision.med.utah.edu.)

backscatter of light and maintains high-fidelity acuity. In contrast, some animals prioritize night vision at the expense of spatial acuity, and in these species the outermost layer of the eye (known as the tapetum) is highly reflective and provides photoreceptors with an additional opportunity to absorb light. (The reflective tapetum is also the reason why a cat's eyes, for example, seem to glow at night.)

Photoreceptors use a highly efficient mechanism to convert a photon of light into an electrochemical neural signal (Fig. 1.3). They contain photopigment, consisting of a membrane protein known as opsin and a chromophore molecule called 11-*cis*-retinal. When light reaches the photopigment, it causes the chromophore's conformation to change from 11-*cis*-retinal to all-*trans*-retinal. All-*trans*-retinal detaches from the opsin molecule because of a low binding affinity. The unbound opsin molecule then activates another membrane complex, the G-protein transducin, by replacing a guanosine diphosphate (GDP) molecule with guanosine triphosphate (GTP) (Palczewski et al., 2000). Activated transducin subsequently stimulates the effector enzyme phosphodiesterase (PDE), which hydrolyzes the cytoplasmic second messenger cyclic guanosine monophosphate (cGMP). Reduction of cytosolic cGMP levels causes membrane sodium channels to close, reducing the inward sodium current and finally causing the cell to become hyperpolarized. As a consequence, the photoreceptor cell reduces its neurotransmitter output in response to the absorption of light. The process is self-limited: the membrane complex transducin catalyzes GTP back to GDP, ceasing stimulation of the PDE enzyme. cGMP levels therefore rise, the inward sodium current is restored, the membrane potential increases, and tonic neurotransmitter release is restored.

In order to maintain the ability for continuous responses to light and preserve high-fidelity neural transmission, it is critical that the photoreceptor responses do not become saturated. Photoreceptors maintain the ability always to produce a signal by ensuring a constant, buffered supply of 11-*cis*-retinal. The spontaneous transformation of all-*trans*-retinal back to 11-*cis*-retinal occurs over a very slow half-life (of several minutes), so that the store of 11-*cis*-retinal is always being replenished and is available to transduce incoming light signals.

Humans possess four photoreceptor types: three cones and the rods. Under most conditions, our vision is mediated by cones, which operate over an enormous range of intensities. Each type of cone photoreceptor has a unique, optimal response to specific wavelengths of light – short (blue), middle (green), or long (red) (Fig. 1.4). Rods, on the other hand, are saturated at natural light intensities and are incapable of discriminating colors; their greater sensitivity to light renders them effective for night vision (scotopic vision). The functional specializations of cones and rods arise from variations in the structure of opsin, since the opsin

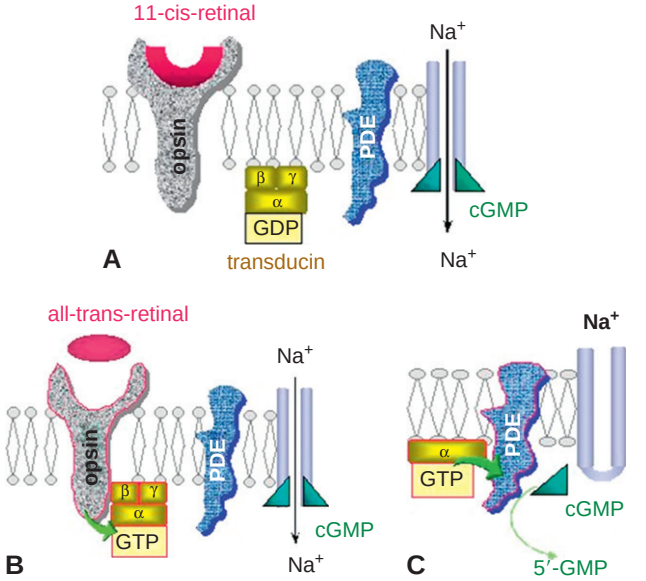

Fig. 1.3. The photoreceptor reaction to light stimulation. (**A**) 11-*cis*-retinal in its inactive state is bound to opsin. (**B**) After absorption of light, the chromophore conformation changes to all-*trans*-retinal and detaches from opsin. Opsin activates transducin by replacing guanosine diphosphate (GDP) with guanosine triphosphate (GTP). (**C**) Activated transducin stimulates phosphodiesterase (PDE), which metabolizes cytosolic cyclic guanosine monophosphate (cGMP). A reduced level of cGMP causes membrane sodium channels to close, lowering the cell's membrane potential and reducing neurotransmitter output. (Reprinted with permission from http://www.lfhk.cuni.cz/rezacovam/fototransmise.)

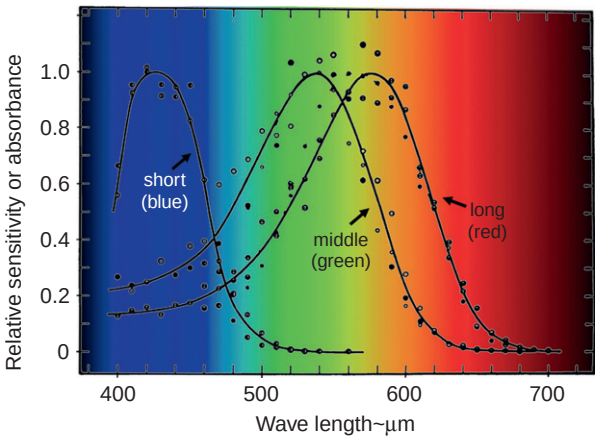

Fig. 1.4. Unique tuning curves for each type of cone photoreceptor (short, middle, and long) at visible wavelengths of light. (Adapted and reprinted with permission from Wald (1964).)

molecule tunes the light wavelengths at which the retinal chromophore (11-*cis*-retinal) will alter its conformation and initiate the biochemical response to light. Despite their functional differences, cones and rods utilize the same 11-*cis*-retinal chromophore.

The amount of signal that a photoreceptor produces depends both on the specific wavelength received and on its intensity. A given photoreceptor may respond equally to a favored wavelength at low intensity and to a less optimal wavelength at high intensity. However, the signal provided by a photoreceptor (the reduction of released neurotransmitters) cannot separately report the dual information of wavelength and intensity. Therefore, downstream cells must distinguish these features of the light stimulus by comparing the different levels of response from each photoreceptor type. The unique response properties of each photoreceptor allow the ratios between their activities to establish the code that resolves this ambiguity.

The distribution of cones and rods across the retina is highly skewed and directly reflects the specialized functions of the fovea and retinal periphery (Osterberg, 1935) (Fig. 1.5). The macula is located temporal to the optic nerve and is approximately 5.5 mm in diameter. Within the macula is the fovea (diameter 1.5 mm) and the foveola (0.35 mm). The fovea has up to 200 000 cones/mm^2 (nearly 15-fold higher than in the peripheral retina) so that it can provide excellent visual acuity (Hirsch and Curcio, 1989). Progressively eccentric locations have much lower concentrations of rods, and thus have decreasing sensitivity. Rods are virtually absent in the fovea; rather, they are the dominant photoreceptor in the periphery.

The neurosensory retina consists of three major layers through which the signal in response to light is transduced: photoreceptors connect to bipolar cells, which relay messages to ganglion cells. In addition, horizontal and amacrine cells form lateral connections between elements of these layers. In the fovea, to support high spatial acuity, each bipolar cell receives input from a single photoreceptor; in contrast, in the retinal periphery a bipolar cell summates the inputs from multiple photoreceptor cells. Bipolar cells then provide inputs to ganglion cells via direct, excitatory glutamatergic synapses or indirect, inhibitory GABAergic connections (Flores-Herr et al., 2001).

The blood supply to the retina arrives via the central retinal artery, which branches off the ophthalmic artery

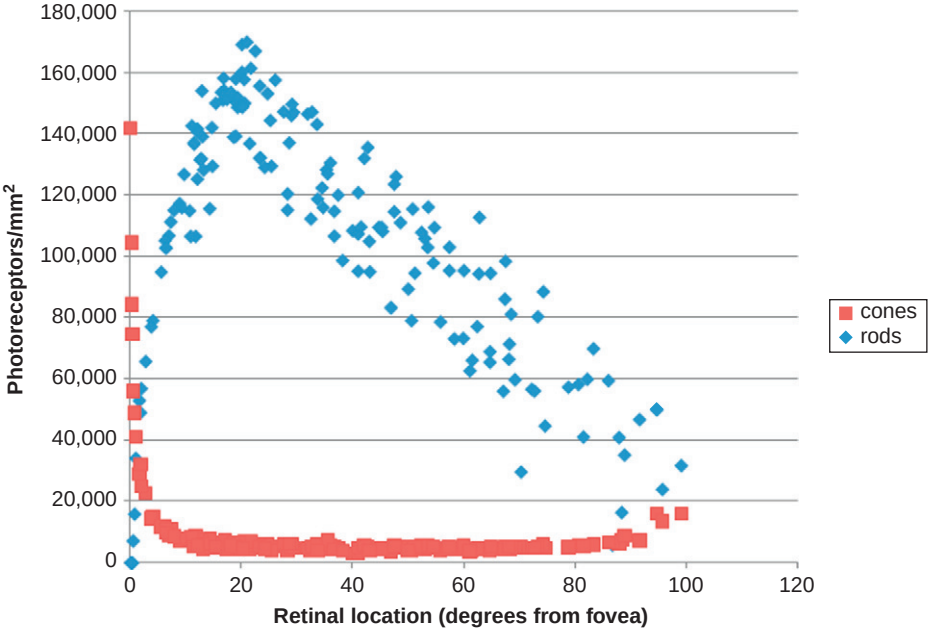

Fig. 1.5. Distribution of rods and cones in the retina. (Adapted from tabulated data (Osterberg, 1935), with permission.)

approximately 1 cm posterior to the globe. It pierces the meninges inferiorly, moves centrally into the nerve, and then emerges in the center of the optic disc (within the optic cup) (Hayreh, 2006). It supplies the inner two-thirds of the retina via temporal vessels that arc above and below the macula within the inner retinal layers. The ophthalmic artery also gives rise to posterior ciliary arteries, which supply the optic nerve head, choroid, and the outer one-third of the retina. A cilioretinal artery exists in about 20% of individuals, arising from the choroidal circulation. In the fovea there is a 400-μm area known as the foveal avascular zone, in which photoreceptors are packed most densely without intervening capillaries.

Retinal veins drain into the central retinal vein, which lies temporal to the central retinal artery in the optic nerve head (Hayreh, 2006). The central retinal vein eventually drains into the superior orbital vein and the cavernous sinus. The choroidal vasculature has a separate drainage route through vortex veins, the superior and inferior orbital veins, and finally into the cavernous sinus.

GANGLION CELLS

The excitatory "on" and "off" inputs to a ganglion cell are arranged to form an antagonistic center-surround receptive field (Kuffler, 1953) (Fig. 1.6). The action potential firing rate of an "on-center" ganglion cell is highest when a light stimulus is in the center of the receptive field, with surrounding darkness. In contrast, the firing rate of "off-center" ganglion cells is highest when a light stimulus is in the peripheral receptive field, but not its center. With uniform illumination throughout a ganglion cell receptive field, the summated center and surround responses essentially cancel each other. However, when differential illumination (i.e., an edge of light) occurs within the receptive field, the imbalance between center and surround inputs allows the ganglion cell to signal the local change in light intensity.

There are three main types of ganglion cell, each with specialized functions in the detection of visual inputs (Table 1.1). Anatomical differences underlie important physiological and functional differences in these types of cell. Eighty percent of ganglion cells are midget cells, 10% are parasol cells, and 10% are other types. The different types of ganglion cells comprise separate pathways that are named for their targets in the LGN. Midget cells form the "P" (parvocellular) pathway and parasol cells form the "M" (magnocellular) pathway (Polyak, 1941; Kaplan and Shapley, 1986; Hendry and Yoshioka, 1994). In addition, small bistratified ganglion cells are the most likely source of a more recently identified "K" (koniocellular) pathway (Hendry and Yoshioka, 1994).

The fovea has a high concentration of midget ganglion cells. Via a narrow dendritic tree, these cells receive signals conveyed by a bipolar cell that has received inputs from a single cone. Midget ganglion cells have cone-opponent receptive fields, allowing spectral selectivity along the red–green or blue–yellow axes. These structural arrangements afford midget ganglion cells the properties of an extremely small receptive field, with specialization for high spatial acuity, color vision, and fine stereopsis (Livingstone and Hubel, 1988).

Parasol ganglion cells, in contrast, receive inputs from multiple bipolar cells, which have sampled several cones. Their presence is greater in the peripheral retina, where the numbers of parasol and midget cells are roughly balanced. At any given retinal eccentricity, parasol cells have a larger receptive field and lower spatial resolution than midget cells due to their broad dendritic arborization (Croner and Kaplan, 1995). Parasol ganglion cells have spatially opponent center-surround organization, allowing edge detection, but they lack spectrally opponent organization; in essence, these cells are color-blind. The anatomical features of parasol cells underlie their specialization for low spatial resolution, motion detection, and coarse stereopsis (Livingstone and Hubel, 1988).

Several other classes of morphologically and physiologically characterized ganglion cell have been identified (Rodieck and Watanabe, 1993). One of

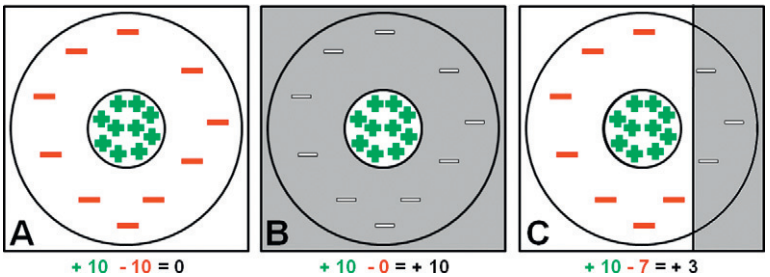

Fig. 1.6. Illustration of "on"-center ganglion cell center-surround organization. White represents stimulation with light and gray represents darkness. (**A**) With diffuse light stimulus in the receptive field, excitatory center and inhibitory surround inputs cancel each other out (in this example, +10 and –10 = 0). (**B**) A narrow beam of light in the on-center elicits maximal response from the ganglion cell (+10 and –0 = +10). (**C**) An edge of light elicits a positive (submaximal) response from the ganglion cell (+10 and –7 = +3).

Table 1.1

Features of the ganglion cell types in the P, M, and K pathways

Property	P pathway	M pathway	K pathway
Retinal source	Midget cells	Parasol cells	Unknown
Receptive field size	Small	Large	Large
Ganglion cells/mm^2	Many	Few	Unknown
Spectral opponency	Yes	No	Some (blue-on)
Conduction velocity of axons	Low	High	Low/varied
LGN projection target	Magnocellular layers	Parvocellular layers	Intercalated
Fraction of LGN population	80%	10%	10%
V1 Projection target	4Cβ	4Cα	Layers 2–3, CO blobs
Illustration			

P, parvocellular; M, magnocellular; K, koniocellular; LGN, lateral geniculate nucleus; CO, cytochrome oxidase.
Illustrations reprinted from Ghosh et al. (1996), with permission.

these, called small bistratified cells, may be the main projection to the koniocellular layers of the LGN (Hendry and Yoshioka, 1994). Relatively little is known about this pathway, because it has been difficult to study in isolation. Given that koniocellular layers of the LGN subsequently project to cytochrome oxidase-rich regions of the upper layers of primary visual cortex (CO "blobs"), these cells may play a role in some aspects of color vision (Hendry and Yoshioka, 1994). An additional class of ganglion cells are unique in that they contain the melanopsin pigment and therefore demonstrate direct responses to light (Hattar et al., 2002). These cells may participate in the pupillary light reflex and may contribute to the pathophysiology of photophobia. Their main function, however, is to mediate circadian rhythms, as discussed below in the section entitled "Suprachiasmatic Nucleus."

The axons of ganglion cells travel in the nerve fiber layer (the innermost retinal layer), enter the optic nerve, travel through the chiasm and tract, and then finally synapse in the LGN of the thalamus. Foveal ganglion cells send axons directly to the temporal aspect of the optic disc in the papillomacular bundle (Fig. 1.7). The remaining temporal ganglion cell nerve axons are arranged on either side of the horizontal raphe and form arcuate bundles that course above and below the fovea, and finally enter the superior and inferior portions of the optic nerve. Finally, axons originating nasal to the disc enter the nasal portion of the optic nerve.

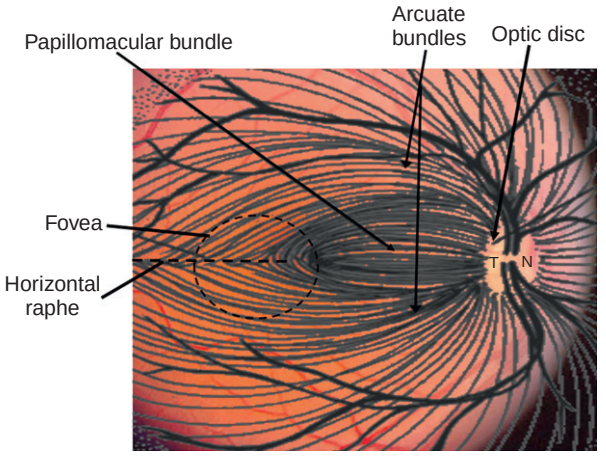

Fig. 1.7. Arrangement of the retinal nerve fiber layer, comprised of ganglion cell axons. The papillomacular bundle conveys axons from the fovea directly to the temporal margin (T) of the optic disc. The remainder of temporal ganglion cell axons are arranged in arcuate bundles above and below the fovea, arriving at the superior and inferior disc margins. Finally, axons originating nasal to the disc arrive at its nasal border (N).

OPTIC NERVE

Each optic nerve is comprised of approximately 1.2 million retinal ganglion cell axons (in constrast to the acoustic nerve, for example, which has only 31 000 axons) (Bruesch and Arey, 1942). The intraocular segment of the optic nerve head (the optic disc) is typically located 3–4 mm nasal to the fovea and is 1 mm thick. The optic disc has a central depression called the optic cup, which is typically one-third the size of the disc (Jonas et al., 1988). There are no retinal photoreceptors in the region of the optic disc, which gives rise to the monocular blind spot (Mariotte, 1668).

The optic nerve travels posteriorly through the lamina cribrosa to exit the back of the globe, where it abruptly increases in diameter from 3 to 4 mm. In order to accommodate the rotations of the globe, the length of the intraorbital segment of the optic nerve is typically between 25 and 30 mm in length, at least 5 mm longer than the distance from the globe to the orbital apex (Glaser and Sadun, 1990). Upon passing through the lamina cribrosa, the optic nerve becomes invested with meninges and also becomes myelinated. Since the optic nerve is an extension of the central nervous system, unlike other cranial and peripheral nerves, it is myelinated by oligodendrocytes rather than Schwann cells. Upon exiting the orbit, the optic nerve enters the optic canal, within the lesser wing of the sphenoid bone, for approximately 6 mm. The intracanalicular optic nerve rises at a 45° angle and then exits the optic canal, where it continues in its intracranial portion for approximately 17 mm before reaching the chiasm.

In the proximal third of the optic nerve the positions of ganglion cell axons are rearranged. Macular ganglion cell axons which initially lie temporally move to the nerve's center. Peripheral temporal fibers become positioned temporally, both superior and inferior to the macular fibers. Finally, nasal fibers remain in the nasal portion of the optic nerve.

Axoplasmic transport is essential to the maintenance of ganglion cell axons (Minckler, 1986). Orthograde axonal transport (movement away from the ganglion cell body, toward the LGN) occurs at both slow and fast speeds, and relies upon elements of the axon cytoskeleton (microtubules, neurofilaments, and microfilaments). Slow transport (1–4 mm/day) is used for elements of the cytoskeleton itself, while fast vesicular transport (400 mm/day) is used for proteins and neurotransmitters, using motor proteins (kinesin and dynein) (Vale et al., 1985). Mitochondria are essential to providing energy in the form of adenosine triphosphate (ATP) for these processes to occur.

All of the blood supply to the optic nerve is ultimately derived from the ophthalmic artery (Fig. 1.8).

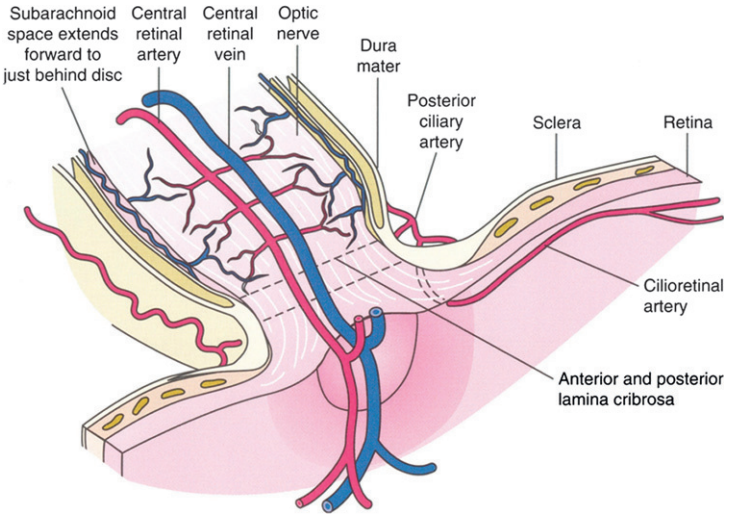

Fig. 1.8. Blood supply to the optic nerve. (Reprinted with permission from Patten (2004).)

The anastomotic circle of Zinn–Haller provides circulation to the optic nerve head, and is supplied by the posterior ciliary arteries, the pial arteriole plexus, and the peripapillary choroid (Anderson, 1970). The posterior ciliary arteries each provide a variable, segmental supply to portions of the optic nerve below its head. Distal portions of the optic nerve receive blood supply from the arterial pial plexus. Within the optic canal, this vascular network is usually supplied by the internal carotid artery, and in the intracranial segment of the optic nerve it is supplied by the internal carotid, anterior cerebral, or anterior communicating arteries.

OPTIC CHIASM

The chiasm, which has a dumbbell shape when viewed in coronal section, is the site of decussation for axons from the optic nerve (Fig. 1.9). It lies in the subarachnoid space of the suprasellar cistern, above the diaphragma sella and the pituitary gland, inferior to the hypothalamus, and anterior to the pituitary stalk (infundibulum). The chiasm is typically 10 mm above the pituitary, which rests in the sella turcica within the sphenoid bone. In most individuals, the chiasm is directly above the pituitary, but in 15% it is displaced anteriorly, above the tuberculum sellae (a prefixed chiasm), and in 5% it is displaced posteriorly, over the dorsum sellae (a postfixed chiasm) (Bergland et al., 1968; Doyle, 1990).

The chiasmal decussation serves to bring together information from the halves of each retina that view the same portion of the visual field. Therefore, axons from nasal ganglion cells cross and join axons from temporal ganglion cells from the contralateral eye. There is a greater number of crossed (53%) than uncrossed (47%) fibers. Among crossing fibers, those originating in the macula lie in a superoposterior position within

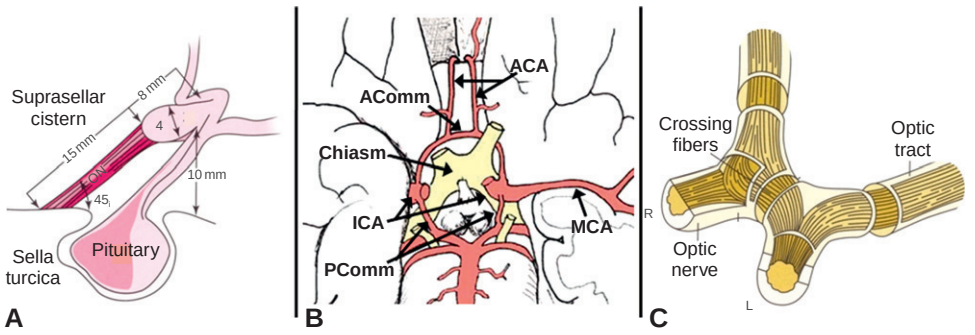

Fig. 1.9. The optic chiasm. (**A**, sagittal view) The chiasm lies in the suprasellar cistern, 10 mm above the pituitary gland in the sella turcica. (**B**, ventral view) The chiasm is situated between the two internal cerebral arteries (ICA). The anterior cerebral arteries (ACA) and anterior communicating artery (AComm) lie superiorly and the posterior communicating arteries (Pcomm) lie inferiorly. (**C**) Partial decussation of ganglion cell axons at the optic chiasm. Inferior nasal fibers decussate anteriorly and superior nasal fibers decussate posteriorly. Temporal fibers travel in the lateral aspect of the chiasm and do not decussate. MCA, middle cerebral artery. (Adapted and reprinted with permission from Hoyt and Luis (1963).)

the chiasm. Axons from the inferior nasal retina may bend slightly forward (up to 3 mm) into the contralateral optic nerve, forming a structure called Wilbrand's knee (Hoyt, 1970). However, the existence of Wilbrand's knee has been questioned, with the suggestion that this anatomical arrangement may be the artifactual result of long-term monocular enucleation (Horton, 1997).

The optic chiasm lies between several main arteries comprising the circle of Willis. It is situated between the two internal carotid arteries at their supraclinoid portion, above the two posterior communicating arteries, and beneath the anterior cerebral arteries and the anterior communicating artery. These neighboring vessels provide an anastomotic supply to the chiasm via an inferior group (the superior hypophyseal arteries, which derive from the internal carotid, posterior communicating, and posterior cerebral arteries) as well as a superior group (branches from the anterior cerebral arteries) (Bergland et al., 1968). The body of the chiasm may be predominantly supplied by the inferior group, whereas the lateral aspects of the chiasm may receive dual supply from both the superior and inferior groups.

OPTIC TRACTS

Each optic tract contains axons from the ipsilateral temporal retina and the contralateral nasal retina. In the proximal optic tract there is a 90° inward rotation of fibers such that inferior retinal axons from each eye become positioned laterally and those from the superior retinas become positioned medially. In the posterior tract, these fibers fan out toward the LGN and interdigitate into its separate layers. The blood supply to the optic tract is variable but typically arises from anastomotic branches of the posterior communicating and anterior choroidal arteries.

LATERAL GENICULATE NUCLEUS

Most fibers from the optic tracts synapse in the ipsilateral LGN. The number of cells in the LGN is large, with nearly a 1:1 ratio to ganglion cell inputs (Spear et al., 1996). There is retinotopic organization in the LGN, with macular vision represented in the hilum (central portion), the superior field represented in the lateral horn, and the inferior field represented in the medial horn (Kupfer, 1962) (Fig. 1.10). The LGN is arranged in six neuronal layers, each with monocular inputs. Ganglion cell axons from the ipsilateral eye (temporal retina) synapse in layers 2, 3, and 5, while axons from the contralateral eye (nasal retina) synapse in layers 1, 4, and 6 (Chacko, 1948). Layers 1 and 2 contain large neurons (magnocellular layers) which receive parasol ganglion cell inputs; layers 3–6 contain small neurons (parvocellular) and receive midget ganglion cell inputs

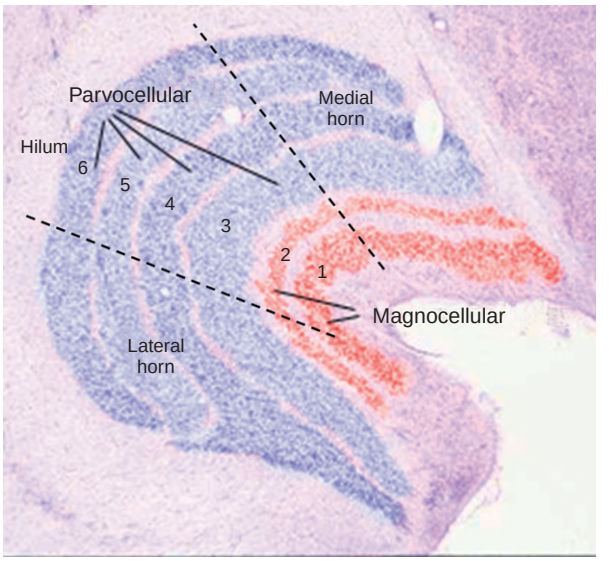

Fig. 1.10. Layers of the lateral geniculate nucleus. Layers 1 and 2 are the magnocellular layers, and layers 3–6 are the parvocellular layers. Inputs to the hilum are from the central visual field, those to the medial horn are from the inferior visual field, and those to the lateral horn are from the superior visual field. (Adapted and reprinted from http://www.psych.ucalgary.ca/PACE/VA-LAB/.)

(Leventhal et al., 1981). In addition, scattered under each of the six major layers of the LGN in an intercalated, intralaminar fashion are the so-called koniocellular (tiny, dust-like) cells.

The blood supply to the LGN is segregated and arrives via the anterior and posterior choroidal arteries. The anterior choroidal artery is a proximal branch of the internal carotid artery, and it supplies the medial and lateral horns of the LGN. The posterior choroidal arteries derive from the posterior cerebral arteries and supply the hilum of the LGN.

The LGN is a critical relay station with dynamic control upon the amount and nature of information that is transmitted to visual cortex (Guillery and Sherman, 2002). In addition to retinal afferents, which may comprise only 5–10% of the synapses in the LGN (Van Horn et al., 2000), the LGN also receives extensive modulating connections from the thalamic reticular nucleus and layer 6 of the visual cortex. The LGN thus provides a bottleneck to information flow, filtering visual information for relevance to the present behavioral state.

The pulvinar is another thalamic nucleus, much larger than the LGN, that forms a higher-order relay receiving extensive descending cortical projections from both layers 5 and 6 of the visual cortex (Chalupa, 1991). While inputs from layer 5 are essential to driving pulvinar responses, inputs from layer 6 have more subtle modulating effects (Sherman and Guillery, 1998). The pulvinar has widespread connections to most cortical regions and is key to

transthalamic corticocortical pathways, capable of modifying transmission in accord with requirements of selective visual attention (Petersen et al., 1987; Rafal and Posner, 1987). More specific functions of the pulvinar in visual processing, however, have yet to be elucidated.

SUPERIOR COLLICULI

The superior colliculi play a critical role in generating orienting eye and head movements to sudden visual (and other sensory) stimuli. They are located in the dorsal midbrain within the tectal plate. The superior colliculi are structurally and functionally organized into superficial and deep layers. The superficial layers solely process visual information, with direct retinal inputs comprising a visuotopic map of the contralateral field (Cynader and Berman, 1972). Along the anterior–posterior axis of each colliculus, the receptive fields of these neurons move from the central visual field to more peripheral locations. Along the medial–lateral axis, the receptive fields move from the upper visual field to the lower visual field. The representation of foveal vision is magnified, with over one-third of collicular neurons processing inputs from the central 10° of vision. The superficial layers have efferent connections to thalamic nuclei; these signals are then relayed to cortical visual areas. The deep layers of the colliculi receive multimodal sensory inputs and help mediate saccadic eye movements through their efferent connections to ocular motor systems. In addition, these layers receive reciprocal connections from several cortical areas involved in generating saccades.

PRETECTAL NUCLEI

A portion of the fibers in the optic tract subserve the pupillary light reflex and synapse at the pretectal nuclei in the midbrain. There is consensual innervation to both pretectal nuclei, and each pretectal nucleus has dual connections to each Edinger–Westphal nucleus. The Edinger–Westphal nuclei give rise to parasympathetic efferent fibers which travel with the oculomotor nerve and regulate pupillary size via pupillary constrictors.

SUPRACHIASMATIC NUCLEUS

A newly identified type of retinal ganglion cell contains the photopigment melanopsin and demonstrates an intrinsic responsiveness to light (not mediated by rod and cone photoreceptors) (Hattar et al., 2002). These ganglion cells give rise to a separate, unmyelinated pathway through the optic chiasm and tracts, ultimately transmitting light information directly to the suprachiasmatic nucleus (SCN) at the base of the anterior hypothalamus (Moore, 1973). As opposed to most visually responsive brain areas, where neural responses are transient, the responses in the SCN are sustained for up to 20 seconds. Together with large receptive fields, these properties allow the SCN to monitor ambient light levels reliably. The SCN has efferent connections to the pineal gland, where melatonin secretion occurs to drive circadian rhythms.

OPTIC RADIATIONS

The second-order neurons of the visual pathway form the optic radiations extending from the LGN to striate (calcarine) cortex in the occipital lobe. These neurons are grouped into two major bundles: the temporal radiations (which take an anterior course through the temporal pole, termed Meyer's loop, before turning in a posterior direction) and the parietal radiations (Van Buren and Baldwin, 1958) (Fig. 1.11). Retinotopic arrangement is maintained; temporal radiations represent the contralateral superior field and parietal radiations represent the contralateral inferior field.

The temporal optic radiations receive blood supply from the anterior choroidal artery as well as proximal branches from the middle cerebral arteries, including the lenticulostriate and inferior temporo-occipital arteries. The parietal radiations are supplied by more distal

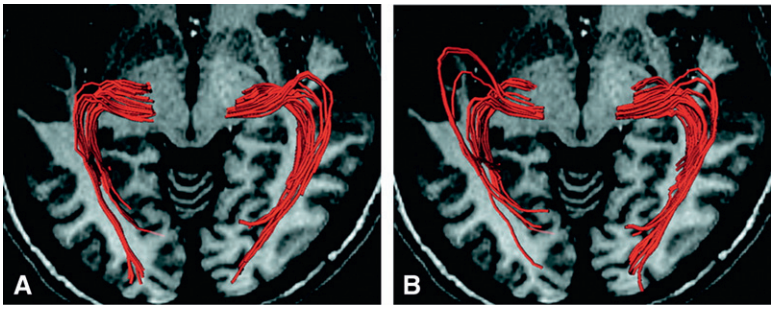

Fig. 1.11. (**A, B**) Pathways of the optic radiations, from the lateral geniculate nucleus to calcarine cortex, demonstrated by diffusion tensor imaging (which identifies white-matter tracts). (Reprinted with permission from Yamamoto et al. (2007).)

branches of the middle cerebral artery, including the angular and posterior temporal arteries. Distal portions of the optic radiations, before their entry into visual cortex, are supplied by the superior temporo-occipital branch of the middle cerebral artery and the anterior temporal and calcarine branches from the posterior cerebral artery.

CALCARINE CORTEX (PRIMARY VISUAL CORTEX)

The optic radiations arrive at the mesial surface of the occipital lobe, in the striate (calcarine) cortex. Fascicles from the parietal radiations synapse in the superior bank of calcarine cortex, while those from the temporal radiations arrive in the inferior bank. These axons make connections in cortical layer 4, termed the "stripe of Gennari," which is plainly visible on gross inspection of the brain (Gennari, 1782). There is a 300–400-fold increase in the total number of neurons in primary visual cortex compared to the retina or the LGN, with approximately 350 million neurons packed at a density that may be twice as high as that in other cortical areas (Tolhurst and Ling, 1988). Representation of the vertical meridian of the visual field lies most medially, in the calcarine lips, while the horizontal meridian is represented deep within the calcarine fissure (Gray et al., 1998; Galetta and Grossman, 2000). Macular projections make their synapses in the posterior pole of calcarine cortex (Fig.s 1.12 and 1.13). The macular representation is greatly magnified in the visual cortex retinotopic map; connections from 1 mm^2 of retina, representing the central 10° (2% of the total visual field), encompass 60% of striate cortex (Tolhurst and Ling, 1988; Horton and Hoyt, 1991). The psychophysical correlate of this cortical magnification is extremely high central acuity (spatial resolution of 60–100 cycles/degree). More anterior portions of striate cortex represent the peripheral visual field. The most anterior bank of calcarine cortex represents the temporal 30° of the

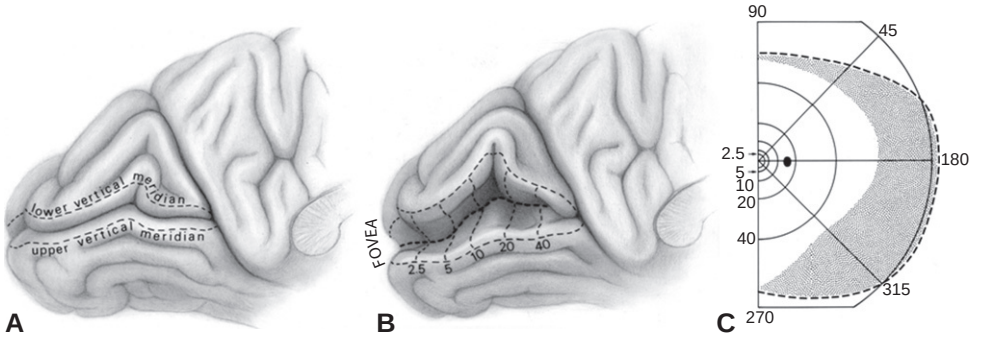

Fig. 1.12. Retinotopic map of the human striate cortex. (**A**) Left occipital lobe, with striate cortex in the lips and banks of the calcarine fissure. The dotted lines demark area V1, showing the upper and lower vertical meridian of the contralateral hemifield. (**B**) The gyrus is lifted to reveal the banks of the calcarine sulcus, with its retinotopic map marked in degrees from the fovea. Note the immense magnification of central vision. (**C**) The contralateral visual field, marked in degrees from the fovea. The dark oval represents the monocular blind spot and the stippled zone represents the monocular crescent. (Reprinted with permission from Horton and Hoyt (1991).)

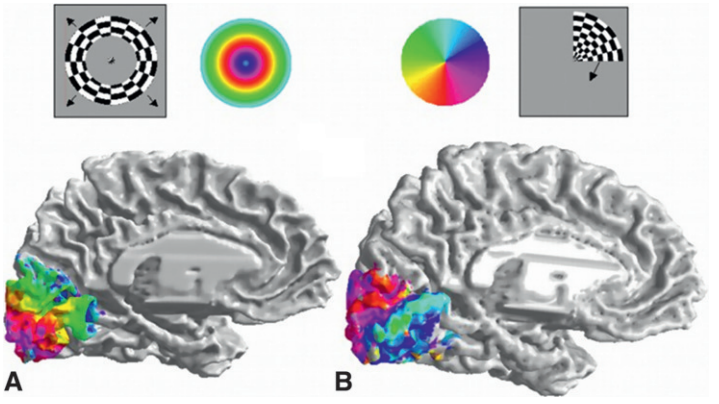

Fig. 1.13. Retinotopic organization of striate cortex using functional magnetic resonance imaging. (**A**) Expanding ring stimuli map receptive field eccentricity. Note magnification of the foveal representation. (**B**) Rotating wedge stimuli map receptive field polar angle. Note that the superior fields are represented in the inferior bank, and the inferior fields are represented in the superior bank. (Reprinted with permission from Dougherty et al. (2003).)

contralateral field; this area receives sole monocular input from the contralateral eye, since this portion of the visual field is not represented by the ipsilateral eye.

The main blood supply to visual cortex is provided by the posterior cerebral arteries and its branches (the calcarine, posterior temporal, and parieto-occipital arteries) (Smith and Richardson, 1966) (Fig. 1.14). At the occipital pole, however, there may be a dual blood supply to the area subserving central vision, with anastomoses between branches of the posterior cerebral arteries and the superior temporo-occipital branch from the middle cerebral artery.

In layer 4 of striate (calcarine) cortex there is anatomical division of the two functionally segregated LGN inputs. Neurons from the magnocellular layers (M pathway) synapse in cortical layer 4Cα, while those from the parvocellular layers (P pathway) synapse in layer 4Cβ. In addition, both M and P pathway neurons send collateral inputs to layer 6, which in turn sends reciprocal projections back to the thalamus. Neurons of the K pathway send projections directly to the "CO blobs" in layer 3 and layer 1 of visual cortex, rather than to layer 4 or 6.

Monocular inputs to primary visual cortex are arranged in ocular dominance columns. The two eyes have different views of visual space, resulting in a slight displacement of their respective retinal images. At the binocular fixation point (which depends upon the amount the eyes are converged), an image is projected on to anatomically corresponding retinal locations. Objects located in front of or behind the binocular fixation point, however, give rise to noncorresponding retinal images (Fig. 1.15). This retinal disparity forms the basis of cortical calculations of stereoscopic depth, since neurons in V1 as well as extrastriate regions are sensitive to these differences. Some cortical neurons respond most strongly for objects further than the fixation point, while others are tuned for objects nearer than the fixation point (Barlow et al., 1967; Poggio et al., 1988; Backus et al., 2001). These features allow the monocular two-dimensional projection of visual space to become a rich, three-dimensional perception (Wheatstone, 1838).

V1 neurons are particularly selective for specific orientations of luminance contrast, forming the basis of image contour analysis (Hubel and Wiesel, 1962). In addition, there is the initial processing of color composition, brightness, and direction of motion (Tootell et al., 1988a, b). The reason that V1 neurons are able to detect contours is that their receptive fields have a larger, elongated on-center that is constructed from the concentric-ring on-center inputs of ganglion cells (Fig. 1.16). When a light stimulus is the preferred orientation, it spans the on-centers of these contributing ganglion cells and therefore elicits a maximal response from the V1 neuron (Hubel and Wiesel, 1962).

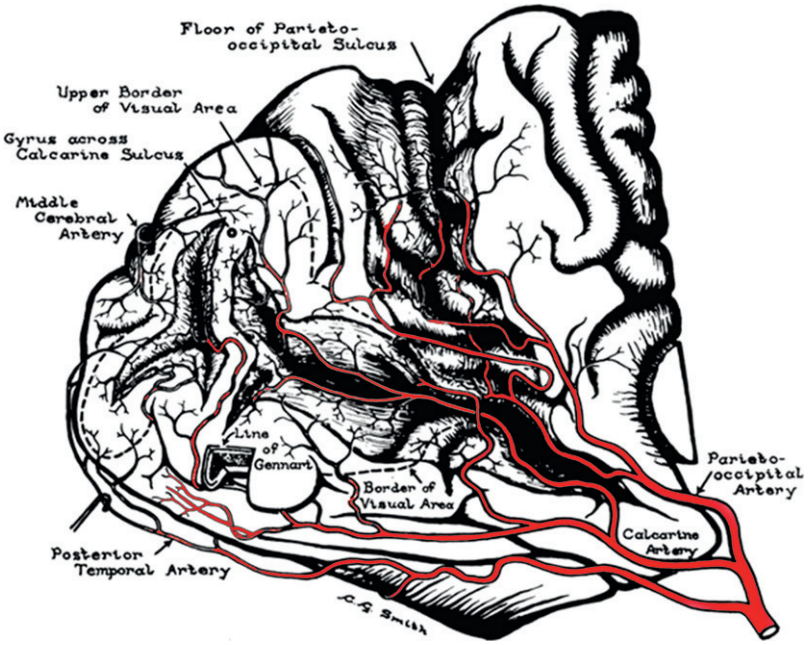

Fig. 1.14. Occipital blood supply. The posterior cerebral arteries provide the majority of the blood supply to the occipital cortex, via the parieto-occipital arteries, calcarine arteries, and posterior temporal arteries. In addition, collateral blood supply to the occipital pole is supplied by branches of the middle cerebral artery, via the superior temporo-occipital arteries. (Adapted with permission from Smith and Richardson (1966).)

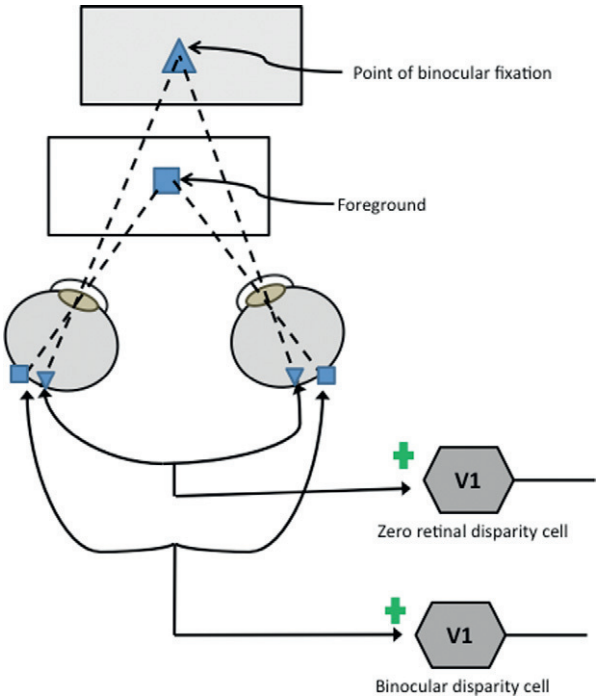

Fig. 1.15. Basis for stereoscopic vision. At the binocular fixation point there is retinal correspondence of images on the fovea, but for objects near or far to fixation there is retinal disparity. Cells in visual cortex are sensitive to the presence and amount of binocular disparity, thus signalling whether images are at the point of fixation or in the fore/background.

FEEDBACK MECHANISMS

Information processing relies not only on feedforward connections to higher visual areas but also on reciprocal connections that transfer information in the reverse direction (Felleman and Van Essen, 1991). These feedback connections, which far outweigh the feedforward inputs arriving from the LGN, serve to fine-tune the processing of incoming stimuli. Even in V1, therefore, neural responses do not mirror retinal inputs precisely, but are modified by higher inputs to support a coherent perceptual interpretation.

While line segments form the ideal stimulus for a V1 neuron given its small, simple receptive field, a single line segment on a blank background is a rarely encountered visual scene. In natural scenes, multiple contour edges are present, forming diverse object boundaries. An accurate perceptual interpretation therefore relies on the contextual processing of individual line segments within the overall visual scene. The context of a stimulus can greatly alter its perceptual salience, with accompanying changes even in early stages of neural processing, including altered responses in V1 neurons themselves (Knierim and van Essen, 1992) (Fig. 1.17). When a stimulus is similar to its surroundings, the camouflage effect is reflected by a reduction of V1 responses corresponding to that receptive field. On the other hand, when a stimulus differs from its surroundings, a perceptual popout occurs, mediated by a partial restoration of V1 responses (Nothdurft, 1991; Knierim and van Essen, 1992). Top-down and horizontal corticocortical connections give rise to contextual modulation in early visual areas by facilitating selective responses (Callaway, 1998). Surrounding stimuli that are outside the "classical" receptive field of a neuron may therefore modulate its activity, through both facilitatory and inhibitory mechanisms (Allman et al., 1985; Lamme and Roelfsema, 2000). In fact, in the right setting, neurons in visual cortex will exhibit responses to illusory contours, which are perceptually suggested

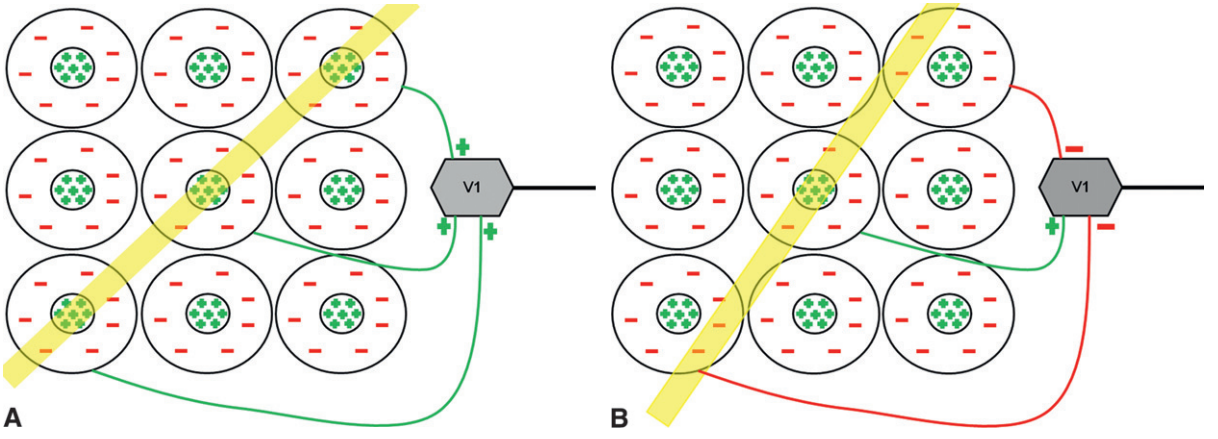

Fig. 1.16. V1 neuron receptive fields. The inputs from adjacent ganglion cells are the inputs to a V1 neuron. (**A**) A light stimulus with the proper orientation will maximally stimulate the V1 neuron. (**B**) A light stimulus with another orientation will create a reduced response from the V1 neuron because of competing excitatory and inhibitory inputs.

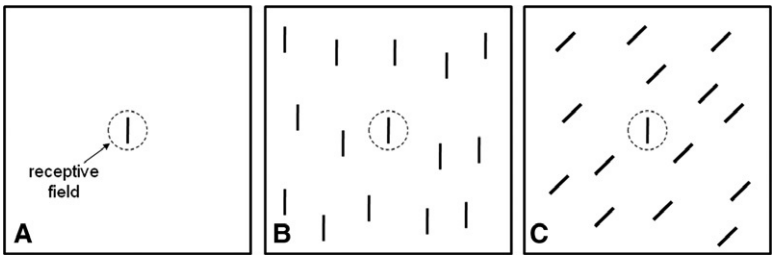

Fig. 1.17. (**A**) The optimal stimulus in the receptive field of a V1 neuron is a line segment. (**B**) The response of the V1 neuron is dampened when many surrounding stimuli contain a similar stimulus (camouflage effect). (**C**) A partial restitution of activity occurs in the V1 neuron when the surrounding stimuli are different from the stimulus processed in its receptive field (popout effect).

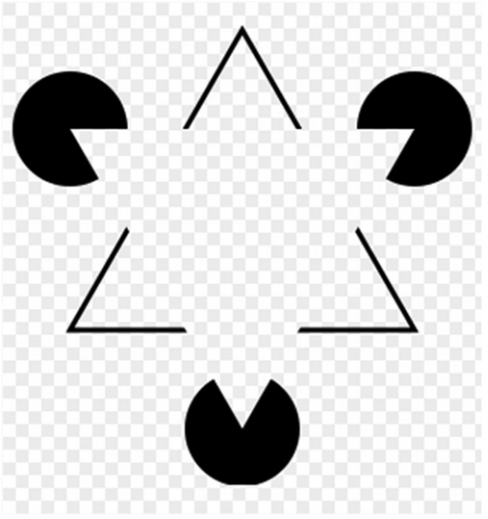

Fig. 1.18. The Kanizsa figure demonstrates the phenomenon of illusory contours. A superimposed white triangle is seen, although no physical stimulus exists to define its shape. Mechanisms of perceptual constancy impose this pattern, with neural firing that supports the coherent perception (Kanizsa, 1976).

by surrounding stimuli but not physically present (von der Heydt et al., 1984) (Fig. 1.18). Ultimately, these mechanisms are essential to generating figure–ground segregation and a coherent phenomenal experience of the visual scene (Lamme et al., 2000).

HIGHER-ORDER VISUAL CORTEX

The complexity of receptive field properties progressively increases from lower-order to higher-order processing areas. Information is integrated to endow higher-order neurons with receptive fields of greatly increased size and complexity. While early processing areas contain neurons with relatively small receptive fields confined to the contralateral visual hemifield, neurons in higher visual areas have expanded receptive fields that span both hemifields. Projections to these higher areas lose their strict point-to-point retinotopic arrangement (Livingstone and Hubel, 1983). Representation of the ipsilateral visual hemifield within these cortical areas is mediated by interhemispheric callosal connections relaying information from contralateral early visual areas.

Multiple extrastriate visual areas, each specialized for the detection of particular attributes of visual scenes, are organized into two roughly parallel processing streams (Fig. 1.19). Ungerleider and Mishkin (1982) originally proposed two functionally dichotomous processing streams, in which the ventral stream mediates visual recognition of objects (the "what" pathway) and the dorsal stream is specialized for processing spatial relationships among objects (the "where" pathway). In addition to visuospatial processing, the dorsal stream is also involved with grasping and manipulating objects (Goodale et al., 1991). The notion of "what" and "where" pathways was built upon an observed double dissociation in the behavior of macaques with selective cortical lesions. Lesions of inferior temporal cortex caused severe deficits of visual discrimination (identifying objects, color, patterns, or shapes) without affecting visuospatial performance

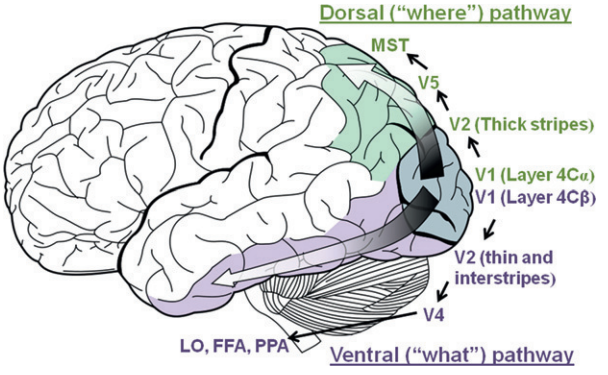

Fig. 1.19. Schematic of the dorsal and ventral processing streams. MST, medial superior temporal area; LO, lateral occipital; FFA, fusiform face area; PPA, parahippocampal place area.

(visually guided reaching or judging the distance between objects); conversely, lesions of posterior parietal cortex had the opposite effects.

The ventral stream begins in layer 4Cβ of area V1, which sends projections to the thin and interstripe regions of V2. The thin region mainly represents color information, while the interstripe regions represent form (Shipp and Zeki, 1985; Sincich and Horton, 2002). These regions subsequently project to area V4 (Zeki, 1980), which ultimately projects to inferotemporal cortex. Here, specialized neurons are involved in visual object processing.

The dorsal stream begins in motion-sensitive components of layer 4Cα in area V1. From here, projections are sent to the thick stripes in areas V2 and V3 (Shipp and Zeki, 1985; Sincich and Horton, 2002). Subsequently, these areas send connections to area V5, and ultimately these inputs arrive at the medial superior temporal area complex, which participates in higher-order motion analysis (Boussaoud et al., 1990; Tootell et al., 1995). Processing in the dorsal stream occurs at shorter latencies than processing in the ventral stream (Schmolesky et al., 1998), leading some investigators to propose the term "fast brain" for the visual areas in the dorsal stream (Nowak and Bullier, 1997). In fact, axons in the dorsal stream contain more myelin than their counterparts in the ventral stream (Nowak and Bullier, 1997).

Functional imaging while subjects perform visual processing tasks has allowed the characterization of highly specialized cortical areas. The lateral occipital (LO) area, within ventral occipitotemporal cortex, has functional specialization for processing objects compared to nonobjects (Tanaka, 1993; Grill-Spector et al., 2001). LO includes the fusiform face area, specialized for face processing (Kanwisher et al., 1997), and the parahippocampal place area, specialized for processing scenes (Epstein and Kanwisher, 1998). Although the retinal inputs of a visual object will differ according to features such as its position, distance, illuminance, and orientation, the ventral stream extracts invariant features of an object that enable perceptual constancy across variable circumstances (Gross and Mishkin, 1977; Ito et al., 1995). Short-term habituation of these neurons, whereby repeated presentations lead to decreased responses, allow signaling of the novelty or significance of an object (Miller and Desimone, 1994).

Ultimately, visual information is sent from both dorsal and ventral streams to distant cortical areas for the highest levels of processing. Inputs to entorhinal cortex (via perirhinal and parahippocampal areas) mediate the formation of long-term memories of visual objects. Inputs to prefrontal cortex are critical for visual working memory. Direct inputs to the amygdala serve to attach emotional valence to a visual stimulus. Mechanisms of attention interact with processing of visual information at all stages (Desimone and Duncan, 1995; Treue and Maunsell, 1996; Reynolds et al., 2000).

CONCLUSION

The visual system demonstrates remarkably efficient organization in its transmission of information with the goal of accomplishing higher-order, complex visuospatial and object identity processing. Anatomical divisions reflect the segregation of functions at each stage. Combined feedforward and feedback connections give rise to powerful computational ability, with high processing efficiency and selective filtering of inputs. The specific anatomical and physiological features of the functional organization of the visual system have been the focus of intense research. Current knowledge has been summarized in this chapter, and further insights are inevitable with ongoing modern research efforts.

References

Allman J, Miezin F, McGuinness E (1985). Stimulus specific responses from beyond the classical receptive field: neurophysiological mechanisms for local-global comparisons in visual neurons. Annu Rev Neurosci 8: 407–430.

Anderson DR (1970). Vascular supply to the optic nerve of primates. Am J Ophthalmol 70: 341–351.

Backus BT, Fleet DJ, Parker AJ et al. (2001). Human cortical activity correlates with stereoscopic depth perception. J Neurophysiol 86: 2054–2068.

Barlow HB, Blakemore C, Pettigrew JD (1967). The neural mechanism of binocular depth discrimination. J Physiol 193: 327–342.

Bergland RM, Ray BS, Torack RM (1968). Anatomical variations in the pituitary gland and adjacent structures in 225 human autopsy cases. J Neurosurg 28: 93–99.

Boussaoud D, Ungerleider LG, Desimone R (1990). Pathways for motion analysis: cortical connections of the medial superior temporal and fundus of the superior temporal visual areas in the macaque. J Comp Neurol 296: 462–495.

Bruesch SR, Arey LB (1942). The number of myelinated and unmyelinated fibers in the optic nerve of vertebrates. J Comp Neurol 77: 631.

Callaway EM (1998). Local circuits in primary visual cortex of the macaque monkey. Annu Rev Neurosci 21: 47–74.

Chacko LW (1948). The laminar pattern of the lateral geniculate body in the primates. J Neurol Neurosurg Psychiatry 11: 211–224.

Chalupa L (1991). Visual function of the pulvinar. In: L Ag (Ed.), The Neural Basis of Visual Function. CRC Press, Boca Raton, pp. 140–159.

Croner LJ, Kaplan E (1995). Receptive fields of P and M ganglion cells across the primate retina. Vision Res 35: 7–24.

Cynader M, Berman N (1972). Receptive-field organization of monkey superior colliculus. J Neurophysiol 35: 187–201.

Desimone R, Duncan J (1995). Neural mechanisms of selective visual attention. Annu Rev Neurosci 18: 193–222.

Dougherty RF, Koch VM, Brewer AA et al. (2003). Visual field representations and locations of visual areas V1/2/3 in human visual cortex. J Vis 3: 586–598.

Doyle AJ (1990). Optic chiasm position on MR images. AJNR Am J Neuroradiol 11: 553–555.

Epstein R, Kanwisher N (1998). A cortical representation of the local visual environment. Nature 392: 598–601.

Felleman DJ, Van Essen DC (1991). Distributed hierarchical processing in the primate cerebral cortex. Cereb Cortex 1: 1–47.

Fishman RS (1973). Kepler's discovery of the retinal image. Arch Ophthalmol 89: 59–61.

Flores-Herr N, Protti DA, Wassle H (2001). Synaptic currents generating the inhibitory surround of ganglion cells in the mammalian retina. J Neurosci 21: 4852–4863.

Galetta SL, Grossman RI (2000). The representation of the horizontal meridian in the primary visual cortex. J Neuroophthalmol 20: 89–91.

Gennari F (1782). De peculiari structura cerebri, nonnolisque ejus morbis. Parmae: Ex Reg. Typog.

Ghosh KK, Goodchild AK, Sefton AE et al. (1996). Morphology of retinal ganglion cells in a new world monkey, the marmoset *Callithrix jacchus*. J Comp Neurol 366: 76–92.

Glaser J, Sadun AA (1990). Anatomy of the visual sensory system. In: J Glaser (Ed.), Neuro-ophthalmology. Lippincott, Philadelphia, pp. 61–82.

Goodale MA, Milner AD, Jakobson LS et al. (1991). A neurological dissociation between perceiving objects and grasping them. Nature 349: 154–156.

Gray LG, Galetta SL, Schatz NJ (1998). Vertical and horizontal meridian sparing in occipital lobe homonymous hemianopias. Neurology 50: 1170–1173.

Grill-Spector K, Kourtzi Z, Kanwisher N (2001). The lateral occipital complex and its role in object recognition. Vision Res 41: 1409–1422.

Gross CG, Mishkin M (1977). The neural basis of stimulus equivalence across retinal translation. In: S Harnard, R Doty, J Jaynes et al. (Eds.), Lateralization in the Nervous System. Academic Press, New York, pp. 109–122.

Guillery RW, Sherman SM (2002). Thalamic relay functions and their role in corticocortical communication: generalizations from the visual system. Neuron 33: 163–175.

Hattar S, Liao HW, Takao M et al. (2002). Melanopsin-containing retinal ganglion cells: architecture, projections, and intrinsic photosensitivity. Science 295: 1065–1070.

Hayreh SS (2006). Orbital vascular anatomy. Eye 20: 1130–1144.

Hendry SH, Yoshioka T (1994). A neurochemically distinct third channel in the macaque dorsal lateral geniculate nucleus. Science 264: 575–577.

Hirsch J, Curcio CA (1989). The spatial resolution capacity of human foveal retina. Vision Res 29: 1095–1101.

Horton JC (1997). Wilbrand's knee of the primate optic chiasm is an artefact of monocular enucleation. Trans Am Ophthalmol Soc 95: 579–609.

Horton JC, Hoyt WF (1991). The representation of the visual field in human striate cortex. A revision of the classic Holmes map. Arch Ophthalmol 109: 816–824.

Hoyt WF (1970). Correlative functional anatomy of the optic chiasm. Clin Neurosurg 17: 189–208.

Hoyt WF, Luis O (1963). The primate chiasm. Details of visual fiber organization studied by silver impregnation techniques. Arch Ophthalmol 70: 69–85.

Hubel DH, Wiesel TN (1962). Receptive fields, binocular interaction and functional architecture in the cat's visual cortex. J Physiol 160: 106–154.

Ito M, Tamura H, Fujita I et al. (1995). Size and position invariance of neuronal responses in monkey inferotemporal cortex. J Neurophysiol 73: 218–226.

Jaffe GJ, Caprioli J (2004). Optical coherence tomography to detect and manage retinal disease and glaucoma. Am J Ophthalmol 137: 156–169.

Jonas JB, Gusek GC, Naumann GO (1988). Optic disc, cup and neuroretinal rim size, configuration and correlations in normal eyes. Invest Ophthalmol Vis Sci 29: 1151–1158.

Kanizsa G (1976). Subjective contours. Sci Am 234: 48–52.

Kanwisher N, McDermott J, Chun MM (1997). The fusiform face area: a module in human extrastriate cortex specialized for face perception. J Neurosci 17: 4302–4311.

Kaplan E, Shapley RM (1986). The primate retina contains two types of ganglion cells, with high and low contrast sensitivity. Proc Natl Acad Sci U S A 83: 2755–2757.

Knierim JJ, van Essen DC (1992). Neuronal responses to static texture patterns in area V1 of the alert macaque monkey. J Neurophysiol 67: 961–980.

Kuffler SW (1953). Discharge patterns and functional organization of mammalian retina. J Neurophysiol 16: 37–68.

Kupfer C (1962). The projections of the macula in the lateral geniculate nucleus of man. Am J Ophthalmol 54: 597–609.

Lamme VA, Roelfsema PR (2000). The distinct modes of vision offered by feedforward and recurrent processing. Trends Neurosci 23: 571–579.

Lamme VA, Super H, Landman R et al. (2000). The role of primary visual cortex (V1) in visual awareness. Vision Res 40: 1507–1521.

Leventhal AG, Rodieck RW, Dreher B (1981). Retinal ganglion cell classes in the Old World monkey: morphology and central projections. Science 213: 1139–1142.

Livingstone M, Hubel D (1988). Segregation of form, color, movement, and depth: anatomy, physiology, and perception. Science 240: 740–749.

Livingstone MS, Hubel DH (1983). Specificity of corticocortical connections in monkey visual system. Nature 304: 531–534.

Mariotte LA (1668). A new discovery touching vision. Phil Trans R Soc Lond 3: 668–671.

Maurice DM (1970). The transparency of the corneal stroma. Vision Res 10: 107–108.

Meyer F (1887). Zur anatomie der orbitalarteien. Morphol Jahr 12: 414–487.

Miller EK, Desimone R (1994). Parallel neuronal mechanisms for short-term memory. Science 263: 520–522.

Minckler DS (1986). Correlations between anatomic features and axonal transport in primate optic nerve head. Trans Am Ophthalmol Soc 84: 429–452.

Moore RY (1973). Retinohypothalamic projection in mammals: a comparative study. Brain Res 49: 403–409.

Nothdurft HC (1991). Texture segmentation and pop-out from orientation contrast. Vision Res 31: 1073–1078.

Nowak LG, Bullier J (1997). The timing of information transfer in the visual system. In: KS Rockland, JH Kaas, A Peters (Eds.), Extrastriate Visual Cortex in Primates, Vol. 12. Plenum Press, New York, pp. 205–241.

Osterberg G (1935). Topography of the layer of rods and cones in the human retina. Acta Ophthalmol 13: 1–103.

Palczewski K, Kumasaka T, Hori T et al. (2000). Crystal structure of rhodopsin: a G protein-coupled receptor. Science 289: 739–745.

Patten J (2004). Vision, the visual fields, and the olfactory nerve. In: J Patten (Ed.), Neurological Differential Diagnosis. Springer, London.

Petersen SE, Robinson DL, Morris JD (1987). Contributions of the pulvinar to visual spatial attention. Neuropsychologia 25: 97–105.

Poggio GF, Gonzalez F, Krause F (1988). Stereoscopic mechanisms in monkey visual cortex: binocular correlation and disparity selectivity. J Neurosci 8: 4531–4550.

Polyak SL (1941). The Retina. University of Chicago Press, Chicago.

Rafal RD, Posner MI (1987). Deficits in human visual spatial attention following thalamic lesions. Proc Natl Acad Sci U S A 84: 7349–7353.

Reynolds JH, Pasternak T, Desimone R (2000). Attention increases sensitivity of V4 neurons. Neuron 26: 703–714.

Rodieck RW, Watanabe M (1993). Survey of the morphology of macaque retinal ganglion cells that project to the pretectum, superior colliculus, and parvicellular laminae of the lateral geniculate nucleus. J Comp Neurol 338: 289–303.

Schmolesky MT, Wang Y, Hanes DP et al. (1998). Signal timing across the macaque visual system. J Neurophysiol 79: 3272–3278.

Sherman SM, Guillery RW (1998). On the actions that one nerve cell can have on another: distinguishing "drivers" from "modulators". Proc Natl Acad Sci U S A 95: 7121–7126.

Shipp S, Zeki S (1985). Segregation of pathways leading from area V2 to areas V4 and V5 of macaque monkey visual cortex. Nature 315: 322–325.

Sincich LC, Horton JC (2002). Divided by cytochrome oxidase: a map of the projections from V1 to V2 in macaques. Science 295: 1734–1737.

Smith CG, Richardson WF (1966). The course and distribution of the arteries supplying the visual (striate) cortex. Am J Ophthalmol 61: 1391–1396.

Spear PD, Kim CB, Ahmad A et al. (1996). Relationship between numbers of retinal ganglion cells and lateral geniculate neurons in the rhesus monkey. Vis Neurosci 13: 199–203.

Tanaka K (1993). Neuronal mechanisms of object recognition. Science 262: 685–688.

Tolhurst DJ, Ling L (1988). Magnification factors and the organization of the human striate cortex. Hum Neurobiol 6: 247–254.

Tootell RB, Hamilton SL, Silverman MS et al. (1988a). Functional anatomy of macaque striate cortex. I. Ocular dominance, binocular interactions, and baseline conditions. J Neurosci 8: 1500–1530.

Tootell RB, Switkes E, Silverman MS et al. (1988b). Functional anatomy of macaque striate cortex. II. Retinotopic organization. J Neurosci 8: 1531–1568.

Tootell RB, Reppas JB, Kwong KK et al. (1995). Functional analysis of human MT and related visual cortical areas using magnetic resonance imaging. J Neurosci 15: 3215–3230.

Treue S, Maunsell JH (1996). Attentional modulation of visual motion processing in cortical areas MT and MST. Nature 382: 539–541.

Ungerleider LG, Mishkin M (1982). Two cortical visual systems. In: DJ Ingle, MA Goodale, RJW Mansfield (Eds.), Analysis of Visual Behavior. MIT Press, Cambridge, pp. 549–586.

Vale RD, Reese TS, Sheetz MP (1985). Identification of a novel force-generating protein, kinesin, involved in microtubule-based motility. Cell 42: 39–50.

Van Buren JM, Baldwin M (1958). The architecture of the optic radiation in the temporal lobe of man. Brain 81: 15–40.

Van Horn SC, Erisir A, Sherman SM (2000). Relative distribution of synapses in the A-laminae of the lateral geniculate nucleus of the cat. J Comp Neurol 416: 509–520.

von der Heydt R, Peterhans E, Baumgartner G (1984). Illusory contours and cortical neuron responses. Science 224: 1260–1262.

Wald G (1933).Vitamin A in the retina. Nature 132: 316.

Wald G (1964). The receptors of human color vision: action spectra of three visual pigments in human cones account for normal color vision and color-blindness. Science 145: 1007–1016.

Wheatstone C (1838). Contributions to the physiology of vision: I. On some remarkable, and hitherto unobserved, phenomena of binocular vision. Philos Trans R Soc Lond 128: 371–394.

Yamamoto A, Miki Y, Urayama S et al. (2007). Diffusion tensor fiber tractography of the optic radiation: analysis with 6-, 12-, 40-, and 81-directional motion-probing gradients, a preliminary study. AJNR Am J Neuroradiol 28: 92–96.

Zeki S (1980). The representation of colours in the cerebral cortex. Nature 284: 412–418.